Launched Waves on a Beam-Plasma System*

C. P. DeNeef, J. H. Malmberg, and T. M. O'Neil
Physics Department, University of California at San Diego, La Jolla, California 92037
(Received 2 March 1973)

An unstable launched wave on a low-density, cold-electron-beam–plasma system grows and traps the beam electrons. Test waves at neighboring unstable frequencies are observed to stop growing where the beam is trapped and to exhibit amplitude oscillations that are coherent with the amplitude oscillations of the main wave. The behavior of the test wave is calculated by regarding it as a slow modulation of the main wave's amplitude and phase.

It is well known that when a low-density, cold electron beam is injected into a collisionless plasma, the nonlinear limit of wave growth occurs because the beam electrons become trapped in the potential troughs of the wave. The local single-wave theory[1-3] assumes that when trapping occurs the wave is monochromatic because the most unstable wave has outgrown the unstable waves at neighboring frequencies. Experiments have shown good agreement with the single-wave theory for the initial nonlinear development of a low-density, cold-beam–plasma system.[4,5] Actually, when the beam is trapped the bandwidth of the statistical beam-grown noise is small, but finite. To investigate the waves within this finite bandwidth, we launch test waves separated slightly in frequency from the main wave (i.e., the fastest-growing wave).[6]

We calculate a test wave's behavior in the nonlinear region by regarding the test wave as a slow modulation of the main wave's initial amplitude and phase. We find agreement with the experimental results.

If we were to calculate the evolution of the test wave by treating it as a separate Fourier component,[7] the calculation would be difficult since the test wave propagates in the presense of the main wave's trapped particle distribution, which is very spatially dependent on both the wavelength and the bounce-length scale. Instead, we regard the test wave as a slow modulation of the main wave's initial amplitude and phase and determine the wave evolution from the single-wave model.[8] Because the electron transit time is short compared to the modulation period, a single electron sees an essentially monochromatic wave (while the spectrum analyzer resolves the frequency separation between the main and test waves).

At the position of the transmitter, the modulated single wave may be expressed as

$$\Phi(t, x=0) = \varphi_0 \exp[i\omega_0 t] + \epsilon\varphi_0 \exp[i(\omega_0 + \Delta\omega)t]$$
$$= C(t) \exp\{i[\omega_0 t + \theta(t)]\},$$

where, to order ϵ,

$$C(t) = \varphi_0 \exp[\epsilon \cos(\Delta\omega t)],$$
$$\theta(t) = \epsilon \sin(\Delta\omega t). \quad (1)$$

We have assumed that the test wave's amplitude is small compared to the main wave's amplitude ($\epsilon \ll 1$). Since we are using the single-wave theory, the modulation must be slow ($\Delta\omega L/u \ll 1$, where L is the system length and u is the beam velocity). The solution for the spatial growth of an *unmodulated* single wave may be expressed in terms of scaled variables as

$$\Phi_L(t, \zeta) = \exp(i\omega_0 t)\Phi_L(\zeta),$$

with

$$\Phi_L(\zeta) = \varphi_0 \exp\{-i\int_0^\zeta [i\kappa_I(\zeta') + \kappa_R(\zeta')]d\zeta'\}, \quad (2)$$

where the scaled universal variables are[8]

$$\zeta = k_0(\eta'/2)^{1/3}x, \quad \kappa = \kappa_R + i\kappa_I = (k - k_0)/k_0(\eta'/2)^{1/3}, \quad \eta' = \tfrac{1}{3}(n_b/n_0)(u/\bar{v})^2.$$

n_b/n_0 is the ratio of beam density to plasma density, and $\bar{v}$ is the thermal velocity of the plasma electrons. ω_0 and k_0 are defined by the two conditions $\omega_0 = k_0 u$ and $\mathrm{Re}[\epsilon(\omega_0, k_0)] = 0$, where $\epsilon(\omega, k) = 0$ is the dispersion relation for the plasma without the beam. In Ref. 2, the universal solution for $\Phi_L(\zeta)$ was computed numerically with ζ and κ represented by τ and Ω, respectively.

The evolution of a single-frequency wave with an arbitrary initial phase $\theta(t)$ and amplitude $C(t)$ is

given by[8]

$$\Phi_{NL}(t,\zeta)=\Phi_L\left(\omega_0 t+\theta(t)+\frac{\kappa_R{}^L}{\kappa_I{}^L}\ln\frac{C(t)}{\varphi_0},\ \zeta+\frac{1}{\kappa_I{}^L}\ln\frac{C(t)}{\varphi_0}\right), \tag{3}$$

where $\kappa_I{}^L=\frac{1}{2}\sqrt{3}$ is the scaled linear growth rate, and $\kappa_R{}^L=-\frac{1}{2}$ is the scaled linear wave number of the wave. Equation (3) simply states that changes in the initial phase and amplitude of the single-wave solution correspond to shifts in the time and space axes.

Receiving this modulated wave through a narrow-band filter corresponds to performing the Fourier transform

$$\Phi_{NL}(\omega,\zeta)=(2\pi)^{-1}\int_{-\infty}^{\infty}dt\,\exp(-i\omega t)\Phi_{NL}(t,\zeta). \tag{4}$$

Equations (1)–(4) lead to the frequency spectrum as a function of distance from the transmitter:

$$\Phi_{NL}(\omega,\zeta)=\Phi_L(\zeta)[\delta(\omega-\omega_0)+\tfrac{1}{2}\epsilon A_+(\zeta)\,\delta(\omega-\omega_0-\Delta\omega)+\tfrac{1}{2}\epsilon A_-(\zeta)\,\delta(\omega-\omega_0+\Delta\omega)+O(\epsilon^2)], \tag{5}$$

where

$$A_\pm(\zeta)=(\kappa_I{}^L)^{-1}\{[\kappa_I(\zeta)\pm\kappa_I{}^L]^2+[\kappa_R(\zeta)-\kappa_R{}^L]^2\}^{1/2}.$$

The functions $\kappa_I(\zeta)$, $\kappa_R(\zeta)$, and $\Phi_L(\zeta)$ are obtained from Ref. 2.

The test wave is the Fourier component at $\omega=\omega_0+\Delta\omega$. The predicted amplitude is linearly proportional to the initial amplitude $\epsilon\varphi_0$, which, as we shall see below, agrees with our experiment. Equation (5) predicts a satellite at $\omega=\omega_0-\Delta\omega$ and linear in $\epsilon\varphi_0$, which we describe below and which has been observed previously.[9] When performed to order ϵ^2, the theory predicts additional satellites at $\omega\pm2\Delta\omega$, which have been observed and interpreted using a different model.[10]

The top curve in Fig. 1 shows the predicted potential of the main wave, computed in Ref. 2, and plotted as a function of the scaled distance along the beam. The lower curves are the predicted potentials of the launched test wave $\Phi(\omega_0+\Delta\omega,\zeta)$ and the satellite $\Phi(\omega_0-\Delta\omega,\zeta)$, computed using Eq. (5) above. The amplitude of the satellite is zero in the linear region, where the launched waves do not interact. The calculation predicts that the test wave will stop growing where the main wave traps the beam.

The apparatus, which has been described elsewhere,[11] produces a 2-m-long, 2-cm-radius plasma column. The effective electron density is 5×10^8 cm^{-3} and the electron temperature is approximately 5 eV. The axial magnetic field is 180 G, so that the plasma frequency (200 MHz) is 0.4 times the cyclotron frequency. The 3-mm radius, 150-V, 200-μA electron beam is produced by an indirectly heated tungsten cathode followed by two Pierce-geometry electron lenses. The ratio of the electron beam density to the plasma effective electron density is 0.01.

Small-amplitude, low-frequency fluctuations in the plasma density and potential cause the frequency of the most unstable wave to fluctuate slightly. In order to fix the frequency of the wave that traps the electron beam, a main wave is launched in the plasma 10–20 dB above thermal noise, using a wire probe. Test waves are launched in the same way at neighboring unstable frequencies and are detected coherently.

It has been known for a number of years that a

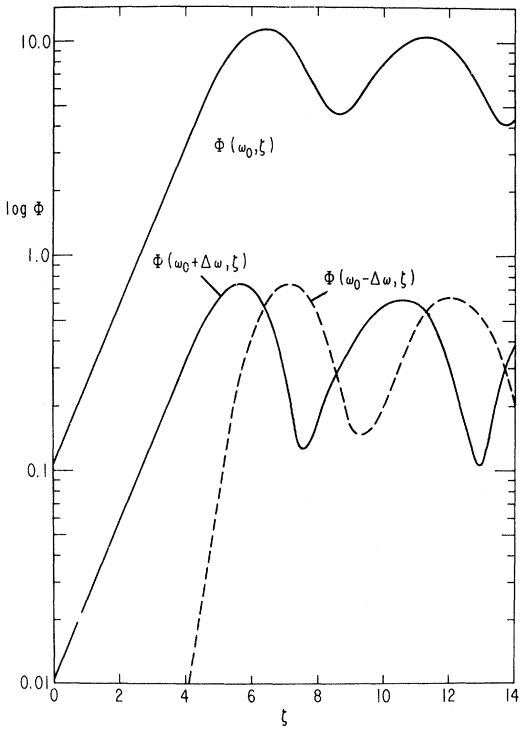

FIG. 1. Top curve, predicted potential of the main wave that traps the beam, computed in Ref. 2 and plotted as a function of the scaled distance along the beam. Lower curves, predicted potentials of the launched test wave $\Phi(\omega_0+\Delta\omega,\zeta)$ and the satellite $\Phi(\omega_0-\Delta\omega,\zeta)$ computed using Eq. (5).

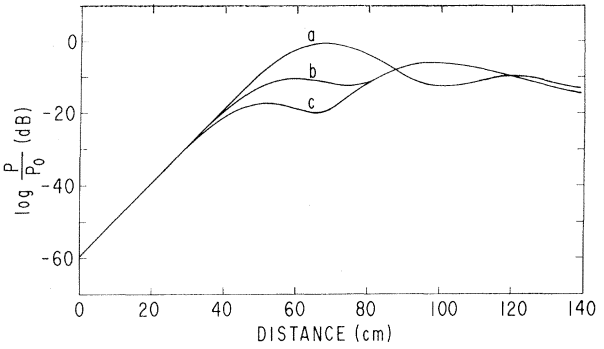

FIG. 2. Received power of a launched wave at 131 MHz as a function of distance from the transmitter. Curve *a*, only the 131-MHz wave is launched. Curve *b*, a larger wave at 127 MHz is also launched. Curve *c*, the amplitude of the 127-MHz wave has been increased.

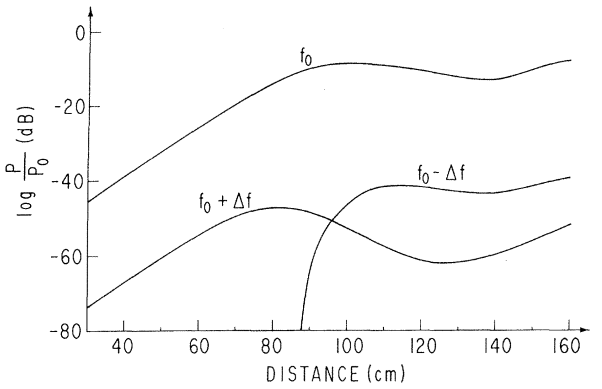

FIG. 3. Received power at each of three frequencies, shown as a function of distance from the transmitter. A large wave is launched with $f_0 = 126$ MHz and a small test wave is simultaneously launched with $f = f_0 + \Delta f = 123$ MHz. No wave is launched at the satellite frequency $f_0 - \Delta f = 129$ MHz.

launched wave on a beam-plasma system suppresses neighboring thermal noise below its natural level.[12] We have observed suppression that is as much as 20 dB over a 10-MHz-wide region of the noise spectrum and is centered on the launched wave frequency. (Our experiments show that a small launched test wave behaves in the same way as unlaunched noise at the test wave frequency.) In the context of the single-wave theory, the launched wave has grown, trapped the beam, and consequently modified the dispersion relation of the unstable waves at neighboring frequencies. Figure 2 shows the received power of a test wave as a function of distance along the beam. Curve *a* shows the test wave launched alone. It grows exponentially (logarithmic scale) until it traps the beam. Then it oscillates as the beam electrons bounce back and forth in the wave troughs as predicted by the single-wave theory. Curves *b* and *c* show the same test wave when a larger wave (not shown) is launched so it traps the beam first. The test-wave growth is unchanged in the linear region until the point where the main wave begins to trap the beam. The test wave's subsequent oscillatory behavior is modified. When the main wave's launched amplitude is increased so that the beam is trapped earlier, the test wave's departure from linear behavior is correspondingly earlier (curve *c*). When the test wave's launched amplitude is varied over 10 dB, its amplitude at all positions is linearly proportional to its launched amplitude. For increases greater than 10 dB, the test wave no longer behaves linearly, probably because the test wave begins to modify the beam dynamics.

Our principal result is the agreement between the experimental data shown in Fig. 3 and the calculation plotted in Fig. 1. The horizontal scale in Fig. 3 is expanded compared to Fig. 1 and extends between $\zeta \approx 2$ and $\zeta \approx 11$. In Fig. 3, $\Delta f = 3$ MHz ($f_0 = 126$ MHz). The results are similar for $\Delta f = 6$ MHz but differ for $\Delta f = 9$ MHz, probably because the assumption $\Delta\omega L/u \ll 1$ is no longer valid.

A sensitive test of the present theory is obtained by predicting and observing the ratio of the amplitude of the test wave to that of the main wave, thus normalizing away departures of the main wave from the prediction of the single-wave theory. Figure 4 is such a comparison between Eq. (5) and the data from Fig. 3 for the test wave (lower curves) and satellite (upper curves). The transformation from actual distance along the beam to scaled units ζ was done by locating the position of the first peak ($\zeta = 6.5$) and measuring the linear growth rate. The test-wave theory and experimental curves were set equal at the beginning of the nonlinear region ($\zeta = 4.0$), corresponding to a measurement of ϵ for use with Eq. (5). The additional breadth of the experimental curves (corresponding to a smearing out of the oscillations in the power curves) may be due to low-frequency fluctuations in the background plasma. The present theory does not include the experiment's time average over an "ensemble" of slightly different plasmas.

In summary, when an unstable launched wave on a low-density, cold-electron-beam–plasma system grows and traps the beam electrons,

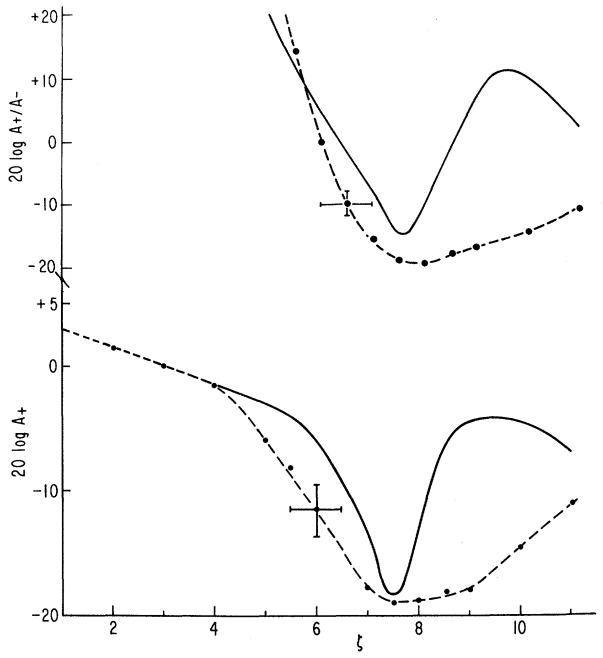

FIG. 4. Bottom curves, ratio of the test wave's amplitude to the main wave's amplitude. Top curves, ratio of the test wave's amplitude to the satellite wave's amplitude. Theoretical curves (solid) obtained using Eq. (5); data (dots and dashed curves) obtained from Fig. 3.

the waves at adjacent unstable frequencies no longer grow according to linear theory. We have observed small test waves at neighboring unstable frequencies and predict their behavior by regarding them as a slow modulation of the main wave's amplitude and phase.

*Work supported by National Science Foundation Grant No. GP-27120.

[1]W. E. Drummond, J. H. Malmberg, T. M. O'Neil, and J. R. Thompson, Phys. Fluids 13, 2422 (1970).

[2]T. M. O'Neil, J. H. Winfrey, and J. H. Malmberg, Phys. Fluids 14, 1204 (1971).

[3]N. G. Matsiborko, I. N. Onishchenko, V. D. Shapiro, and V. I. Shevchenko, Plasma Phys. 14, 591 (1972).

[4]K. W. Gentle and C. W. Roberson, Phys. Fluids 14, 2780 (1971).

[5]K. Mizuno and S. Tanaka, Phys. Rev. Lett. 29, 45 (1972).

[6]Similar observations have recently been reported by W. Carr, D. Bollinger, D. Boyd, H. Liu, and M. Seidl, Phys. Rev. Lett. 30, 84 (1973).

[7]W. L. Kruer, J. M. Dawson, and R. N. Sudan, Phys. Rev. Lett. 23, 838 (1969).

[8]T. M. O'Neil and J. H. Winfrey, Phys. Fluids 15, 1514 (1972).

[9]J. Chang, M. Raether, and S. Tanaka, Phys. Rev. Lett. 27, 1263 (1971).

[10]W. Carr, D. Boyd, H. Liu, G. Schmidt, and M. Seidl, Phys. Rev. Lett. 28, 662 (1972).

[11]J. H. Malmberg and C. B. Wharton, Phys. Fluids 12, 2600 (1969).

[12]A. Bouchoule, M. Weinfeld, and S. Bliman, in *Third European Conference on Controlled Fusion and Plasma Physics, Utrecht, The Netherlands, 1969* (Wolters-Noordhoff Publishing, Groningen, The Netherlands, 1969), p. 26.

Model of Parametric Excitation by an Imperfect Pump*

E. J. Valeo and C. R. Oberman
Plasma Physics Laboratory, Princeton University, Princeton, New Jersey 08540
(Received 19 March 1973)

We examine the three-wave decay instability due to a monochromatic pump with a phase which undergoes a random walk with diffusion coefficient D. Analytic results are obtained for small and large D/γ_0 (where γ_0 is the growth rate for $D=0$), which demonstrate, respectively, a fractional reduction of γ by D/γ_0 and a growth rate γ_0^2/D. Results are also presented for intermediate values of D/γ_0.

It is now clear that parametric instabilities play a crucial role in the interaction of intense radiation with plasma.[1] Some of the effects are desirable, such as the anomalous absorption and concomitant heating in confined plasmas. However, in the laser-pellet interaction, this heating, if untimely, may prove troublesome for fusion prospects.[2] In addition the presence of the Raman and Brillouin backscattering instabilities[3] in the highly underdense region may, theoretically at least, isolate the core of the pellet from the radiation.

Because of the resonant nature of some of these instabilities, any mechanism which causes